Raman and Luminescence Spectra of Dianthracene at High Pressures

BY YUKIKO EBISUZAKI

Department of Chemistry, North Carolina State University,
Raleigh, North Carolina 27607

AND

THOMAS J. TAYLOR, JOHN T. WOO AND MALCOLM NICOL†*

Department of Chemistry, University of California,
Los Angeles, California 90024

Raman spectra of single crystal and powdered samples of dianthracene have been recorded at temperatures from 77 to 410 K and at pressures to 32 kbar. The Raman and infrared spectra of dianthracene dispersed in KBr demonstrate the apparent stability of dianthracene under these conditions, contrary to other reports. At pressures above 10 kbar, however, a fluorescence background appeared with the Raman spectra excited with Ar and He–Ne lasers. This fluorescence is attributed to direct excitation of close-coupled sandwich-like dimer defects created and trapped in the crystal under pressure.

The photodimerization of anthracene in both the solid state and solution is well known.[1-3] The relationship between anthracene and dianthracene is of fundamental interest, and considerable research has been reported on the excited intermediary state and on the role of topochemical factors in the dimerization.[3-13] However, very few physical properties of the dimer have been described, other than that it is unstable at high temperatures and under compression.[5-7, 13] This study was motivated by the interest as to whether the monomer or the dimer is the stable form at high pressures and by the fact that the Raman spectrum of dianthracene does not appear to have been reported. This work attempts to characterize the principal features of the Raman and infrared spectra and to employ the former as a probe to study the stability of dianthracene under static compression to 32 kbar. The luminescence background observed in the Raman studies at high pressures using 547.9, 488.0, 514.5 and 632.8 nm laser excitations is also reported.

In the dimerization process, two anthracene molecules are joined at the 9 and 10 position as shown in fig. 1.[14, 15] The two original anthracene molecules have lost their planarity, and bonds close to tetrahedral arrangement are formed at C_9 and C_{10} positions. The resulting dimer looks like two anthracene " butterflies " facing each other. The bond distance (C_9—$C_{9'}$ and C_{10}—$C_{10'}$) of 1.62 Å between the two anthracene components is much larger than the usual single bond value of 1.55 Å. This is believed to arise from the repulsive forces that hinder the close approach of the two half-molecules. Despite the large C—C distance, the dimerization gives rise to a 2.7 % volume contraction. The dimer in fig. 1 has D_{2h} molecular symmetry and crystallizes to form an orthorhombic structure of $D_{2h}^{15}(P_{bca})$ space group. The four

† Alfred P. Sloan Foundation Fellow.

dimer molecules of the primitive cell have different orientations and are situated on C_i sites. In this symmetry, the librational motions along the three principal axes of each molecule give rise to twelve Raman active motions, three each of A_g, B_{1g}, B_{2g} and B_{3g} species. All 276 possible internal modes of *gerade* character are also Raman active. Fortunately, many internal modes are either accidently degenerate or too weak to detect. The infrared active modes are of the B_{1u}, B_{2u} or B_{3u} type; modes of A_u symmetry are inactive.
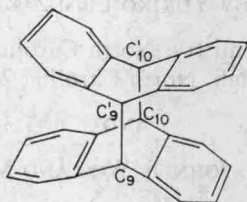

FIG. 1.—The structure of the dianthracene molecule.

The photodimerization mechanism of anthracene and other anthracene derivatives involves the encounter of a molecule in its first excited singlet state with another in its ground state.[4, 5, 16] It is commonly believed that the excimer is the excited intermediary complex. Ideal conditions for the formation of an excimer must be met if the reaction is to proceed through the photoassociated state. The experimental studies on the relationship between crystal structure and fluorescence have shown that most planar aromatic molecules are capable of forming an excimer when there is sufficient coupling between adjacent molecules in an appropriate geometry.[17, 18] In crystalline anthracene, the geometric and coupling requirements are not ideal; however, this crystal indicates unexpected photoreactivity. Owing to these difficulties, many investigators have turned to the study of the photodecomposition process in dianthracene for obtaining information on the dimerization process. The primary step in the photodegradation of the dimer is believed to provide a sandwich or pair-wise arrangement in which the intermolecular spacing is small enough for large intermolecular coupling. The sandwich modification, stable only at low temperatures, exhibits excimer fluorescence. The sandwich-like structure has also been interpreted to be consistent with the anthracene fluorescence under pressure.[9, 19-21]

EXPERIMENTAL

Synthetic anthracene (Eastman H480) was the starting material for photodimerization of anthracene in cyclohexane solution. A solution of anthracene in a Pyrex tube was degassed by the freeze–thaw technique and was irradiated in a photochemical Hg vapour reactor until the characteristic purple luminescence from anthracene was no longer visible and fine white powder of dianthracene was obtained. The powder was washed in cyclohexane and was vacuum dried. Cyclohexane was the preferred solvent since dianthracene samples prepared in benzene required considerably more effort to remove the residual anthracene and benzene. Dimer prepared in cyclohexane and benzene gave identical Raman spectra with no observable monomer peaks. Dianthracene was also prepared from anthracene (Eastman X480) of different purity from that of the basic sample in order to check for possible impurity effects on the high pressure luminescence spectra. Dianthracene-d_{20} was prepared from anthracene-d_{10} (Merck, Sharp and Dohme of Canada) dissolved in nondeuterated cyclohexane solution; the contamination by the nondeuterated dimer was believed to be quite small since no C—H stretching frequency could be detected in the Raman spectrum,

Solubility of dianthracene is very low in most solvents; large crystals are difficult to grow. Small crystals with surface area of $\sim$ 2 mm², however, were grown from chlorobenzene and benzene solution, with the former solvent being preferred. Microscopic examination indicated very clear and well-developed crystals. Only crystals were employed in the high pressure luminescence work, although both powder and crystals were used in the Raman scattering studies.

The near infrared (600 to 3500 cm⁻¹) spectrum at atmospheric pressure and 296 K was obtained with a Perkin–Elmer Model 421 spectrometer, using both the KBr pellets and Nujol mulls. No pulverization of the dianthracene powder was required in making the mulls or the pellets since the sample synthesized in cyclohexane was in a finely divided state. The pellets were prepared by standard KBr technique and were only pressed for a short duration at 4 kbar. Both the pellet and the mull gave identical infrared bands.

Raman data were taken with 90° geometry using a Spectra Physics (Model 165) argon ion laser (200 to 400 mW) operating at 514.5 nm in conjunction with a Spex double monochromator and ITT FW 130 photomultiplier operated in a photon-counting mode. No correction for photomultiplier response with varying wavelength was made in any of the reported spectra. All Raman spectra of dianthracene and dianthracene-d_{20} recorded at atmospheric pressure were obtained on samples sealed under vacuum in Pyrex tubes. Detailed studies of the complete Raman spectra were carried out at atmospheric pressure and in the 296 to 410 K temperature range, while only the lattice modes were examined at lower temperatures to 77 K. The high pressure Raman spectra of both the internal and the lattice modes of the dimer were obtained with the sample placed in the cavity in a NaCl crystal inside the high pressure chamber of a Drickamer type I cell. The pressure studies were carried out to 32 kbar at 296 K. The Raman scattering from dianthracene was sufficiently strong that a scan rate of several cm⁻¹ min⁻¹ and a 1 cm⁻¹ resolution could be maintained in all regions of the spectrum.

The luminescence background observed in the high pressure Raman spectra were studied with the Raman apparatus already mentioned, however a much faster scanning rate was employed with this work. The luminescence spectra were excited with a Spectra–Physics Model 125 He–Ne laser (632.8 nm) and with the various lines of the argon ion laser (457.9, 488.0, and 514.5 nm), but at no time was the sample exposed to the full power of 488.0 and 514.5 nm beam. No attempt was made to " scramble " either the incident or the emitted light since the stressed NaCl windows in the high pressure cell are quite effective as polarization " scramblers ". The spectra were investigated both as a function of irradiation time and pressures to 32 kbar at ambient temperatures. A Molectron Model UV-100 nitrogen laser and Model DL-200 dye laser combination were employed at 488.5 nm to obtain the luminescence spectrum for lifetime studies. The emission was isolated with a narrow band interference filter (514.5 ± 3.0 nm) and a 0.25 m Bausch and Lomb high intensity monochromator. A RCA 1P28 photomultiplier was employed for detection and the spectrum was displayed on an oscilloscope (Tektronix Model 7904). The fluorescence lifetime was determined by comparison of the photographic traces of the excitation and fluorescence.

RESULTS

The near infrared spectrum of the dimer taken on a KBr wafer is shown in fig. 2, and the wavenumbers of the bands are listed in table 1. The KBr disc was prepared from powdered dimer synthesized in cyclohexane. Comparison of the dimer spectrum with the standard anthracene spectrum shows the absence of characteristic anthracene bands.[22] The process of dispersing dianthracene in powdered KBr and pressing a pellet at 4 kbar did not cause any appreciable decomposition, and also any anthracene coprecipitated with the dianthracene must be quite small. The infrared spectrum in fig. 2 agrees with the major characteristic bands reported for a mixed monomer–dimer sample and verifies that the samples employed in this work are identical to the dimer reported previously.[7]

Fig. 3 depicts a typical Stokes Raman spectrum of dianthracene powder at atmospheric pressure and 296 K and excited by 514.5 nm radiation. The spectrum shows no visible luminescence under these conditions. The Raman frequencies obtained on small crystals were identical to those of powdered samples; however, the
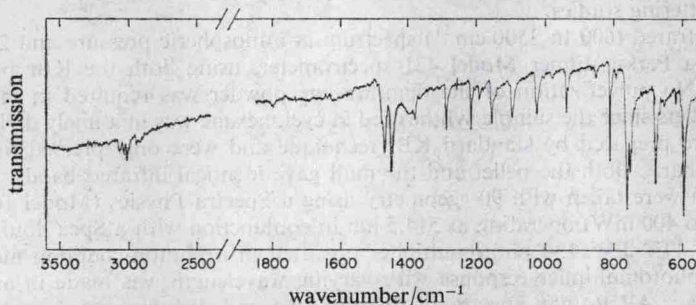

FIG. 2.—A near infrared spectrum of dianthracene at 1 bar and 296 K. The spectrum was taken with dianthracene powder in a KBr pellet pressed at 4 kbar.
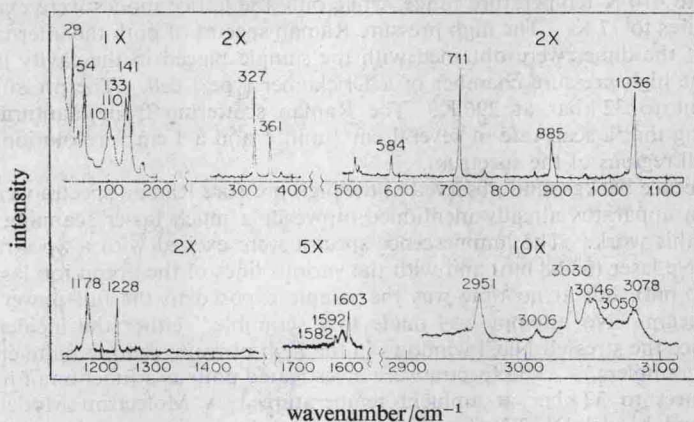

wavenumber/cm⁻¹

FIG. 3.—Raman spectrum of dianthracene powder at 1 bar and 296 K.

TABLE 1.—WAVENUMBERS (cm⁻¹) OF THE NEAR INFRARED BANDS IN DIANTHRACENE AT 1 bar AND 296 K

595	940	1287	[2918]
678	1026	1380	[2944]
752	1096	1394	3014
762	1154	1447	3035
812	1194	1465	3065
937	1216	1795	

[   ] values with large uncertainty

relative intensities were somewhat different owing to the orientation effect of the crystals. The wavenumbers of the 54 observed peaks (due to 11 lattice and 43 internal modes) are given in table 2 together with a partial assignment based on characteristic frequencies and isotope shifts; the molecule is too complex and the spectral identification too incomplete to justify a more detailed assignment at this time. A comparison of the Stokes and anti-Stokes spectra confirmed that all reported bands correspond to vibrational Raman spectra. Examination of the

infrared and the Raman bands in dianthracene (table 1 and 2) indicate no coincidence in the wavenumbers of peaks with appreciable intensity with the possible exception of the band at 3065 cm⁻¹. Since coincidence of wavenumber is excluded for this crystal symmetry, the mode at 3065 cm⁻¹ is assigned as a combination. The division

TABLE 2.—BANDS OF THE RAMAN SPECTRUM OF DIANTHRACENE AT 296 K

wavenumber/cm⁻¹ (1 bar)	intensity [a] (1 bar)	wavenumber/cm⁻¹ (10 kbar)	$\frac{d\nu}{dP}$/cm⁻¹ kbar⁻¹	assignment
		lattice modes		
28.₅	vs	37	0.73	libration
37.₁	m	55	1.6	
53.₆	vs	73	1.9	
71.₃	w, br	91	2.0	
[91] [b]	m, sh	103	1.6	
101	s	120	1.9	
110	s	138	2.8	
133	vs	147	1.4	
141	vs	166	2.6	
167	m	185	1.8	
172	m	192	2.0	
		internal modes		
258	vw			
327	vs	339	1.2	(C—C deformation)
361	m	365	0.52	
378	vw	384	+	
510	m	516	+	
516	w	525	+	
[555]	vw			
584	m	586	+	
[637]	vw			
711	vs	717	0.5	(aromatic C—C stretch–bend)
760	vw	770	+	
[820]	vw			
851	vw		+	
885	m	889	+	
890	m, sh	896	+	
950	vw	956	+	
[996]	vw			
[1024]	vw, sh			
1036	m, sh			
1038	vs	1041	0.46	
1158	w			
1178	s	1176	−0.18	
[1187]	w, sh	1189	0.2	
1200	w	1206	0.5	
1228	s	1236	0.6	
1246	vw		+	
1263	vw	1268	+	
1265	vw	(unresolved)	+	
[1302]	vw			
1320	vw			
[1338]	vw			
1464	vw			

TABLE 2.—contd.

wavenumber/cm^{-1} (1 bar)	intentisy ^{a} (1 bar)	wavenumber/cm^{-1} (10 kbar)	$\frac{d\nu}{dP}$/cm^{-1} kbar^{-1}	assignment
1582	vw	1588	0.7	(aromatic C—C ring stretch)
1592	vw, br	1599	0.7	
1603	w	1613	1.1	
2951	w, br	2971	2.0	(aliphatic C—H stretch)
3006	vw, br	3020	1.4	(aromatic C—H stretch)
3022	vw, sh			
3030	w	3041	1.2	
3046	w, br	3058	1.2	
3050	w, br	3076	2.6	
3065	w, br			
3078	w, br	3099	2.1	

^{a} The following abbreviations have been used: s, strong, m, medium; v, very; w, weak; br, broad; sh, shoulder. ^{b} [   ] values with large uncertainty.

between the lattice and the internal modes in dianthracene is placed at the 175-258 cm^{-1} wavenumber gap. Although this division is rather arbitrary, the smallness of the isotope effect (table 3) for the low frequency librational modes, their large **wavenumber** shift (dν/dP) with pressure, and finally a comparison of the present results with those on benzene and other aromatics support this division.[23-25] The spectrum of the low frequency peaks at 77 K indicates that the lattice phonons reported in table 2 all appear to arise from one-phonon processes.

The spectrum of dianthracene-d$_{20}$ powder is shown in fig. 4, and the wavenumbers of the Raman bands reveal several interesting changes in the number of observed peaks and in the relative intensity in several spectral regions. For example, the central (1569 cm^{-1}) of the three peaks in the ring carbon–carbon stretch region (1500-to-1600 cm^{-1}) of dianthracene-d$_{20}$ is the strongest, while the highest wavenumber mode at 1603 cm^{-1} is the strongest in the nondeuterated compound. This intensity shift may very well arise from Fermi-resonance phenomena in a manner similar to that observed in benzene.[23] Unlike the benzene case, however, no significant change of intensity could be observed when interatomic distances were changed with pressure (fig. 5 and 7). In the spectral region of the aromatic carbon–hydrogen stretch (3000-to-3100 cm^{-1}) of dianthracene, seven peaks are resolved of which the 3030 cm^{-1} peak is most intense. In dianthracene-d$_{20}$, only three peaks are resolved in the aromatic C—D stretch region with the highest wavenumber band (2290 cm^{-1}) being most intense. One possible reason for the change in the number of bands in the carbon–hydrogen stretching region is the removal of combination peaks upon deuteration, while the change in the intensity change can arise from Fermi resonance.[23] In the lower wavenumber region, the intensity of the peak at 327 cm^{-1} is larger than that at 361 cm^{-1} in dianthracene; on the other hand, an apparent reversal of intensity occurs in dianthracene-d$_{20}$ where the 336 cm^{-1} peak becomes stronger than that of the peak at 306 cm^{-1}. The large asymmetry of the 1178 cm^{-1} peak in dianthracene was used as a guide to locate the corresponding peak (1126 cm^{-1}) in dianthracene-d$_{20}$. This mode is assigned as a C—C ring vibration. Deuteration affects only the wavenumber, and there is no change in the relative position, intensity or in the line shape for the low-wavenumber lattice modes. When heated from 296 to 410 K, the dianthracene bands, especially the lattice modes,

decrease in intensity with increasing temperature until it becomes difficult to follow the spectrum beyond 410 K. Other than this intensity decrease, which is typical of organic compounds, no unusual temperature dependent anharmonicity such as a large change in the line shape, relative intensity or extremely large frequency decrease could be observed in the temperature span covered. No background luminescence was apparent in the high temperature Raman spectra excited by 514.5 nm; that is to say, no indication of dissociation to loosely associated pairs of anthracene molecules was detected either by the appearance of new Raman bands or of a fluorescence emmision.

TABLE 3.—BANDS OF THE RAMAN SPECTRUM OF DIANTHRACENE-d_{20} AT 296 K AND 1 bar

| modes of dianthracene-d_{20} | | corresponding modes of dianthracene | |
wavenumber/cm^{-1}	intensity [a]	wavenumber/cm^{-1}	ν_H/ν_D
lattice modes			
$27._4$	vs	$28._5$	1.04
$36._3$	vs	$37._1$	1.02
$51._9$	vs	$53._6$	1.03
$66._9$	w	$71._3$	1.07
$88._8$	m	[91] [b]	1.02
$98._0$	s	101	1.03
105	s	110	10.5
[119]	m		
130	vs	133	1.02
135	vs	141	1.04
153	m	167	1.09
158	m	172	1.09
internal modes			
306	s	327	1.07
336	vs	361	1.07
351	w		
466	w		
558	w		
607	vw		
671	vs	711	1.06
802	vw		
803	w		
856	vs, br	885	1.03
872	w, sh	890	1.02
924	vw		
955	s		
986	m		
1117	m, sh		
1126	vs	1178	1.05
1210	m	1228	1.01
1549	vw	1582	1.02
1569	m	1603	1.02
1583	vw	1592	1.01
2184	w		
2208	w	2951	1.34
2261	m	3030	1.34
2272	vw		
2290	s	3078	1.34

[a] The following abbreviations have been used: s, strong; m, medium; v, very; w, weak; br, broad; sh, shoulder. [b] [ ] values with large uncertainty.

The pressure dependence of both the internal and the lattice modes was studied at 296 K. Table 2 also lists the values of the wavenumbers of the observed peaks at 10 kbar, while the spectrum is shown in fig. 5. Plots of wavenumber against pressure are not quite linear; therefore, only the initial slopes $(\mathrm{d}\nu/\mathrm{d}P)$ are tabulated
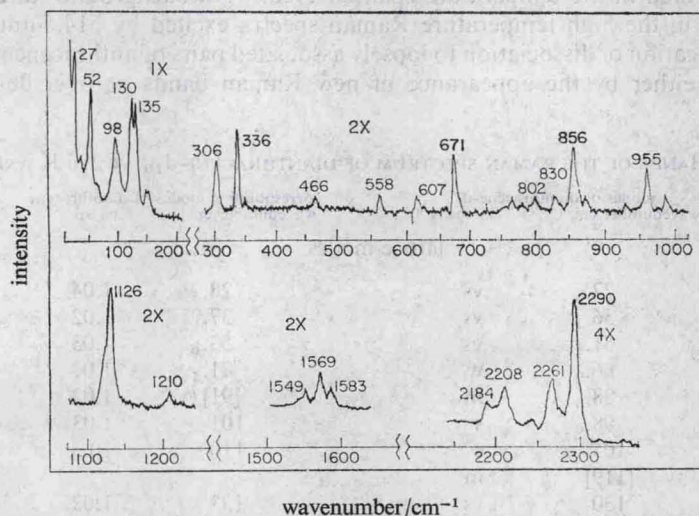

wavenumber/cm^{-1}

FIG. 4.—Raman spectrum of dianthracene-d$_{20}$ powder at 1 bar and 296 K.

wavenumber/cm^{-1}
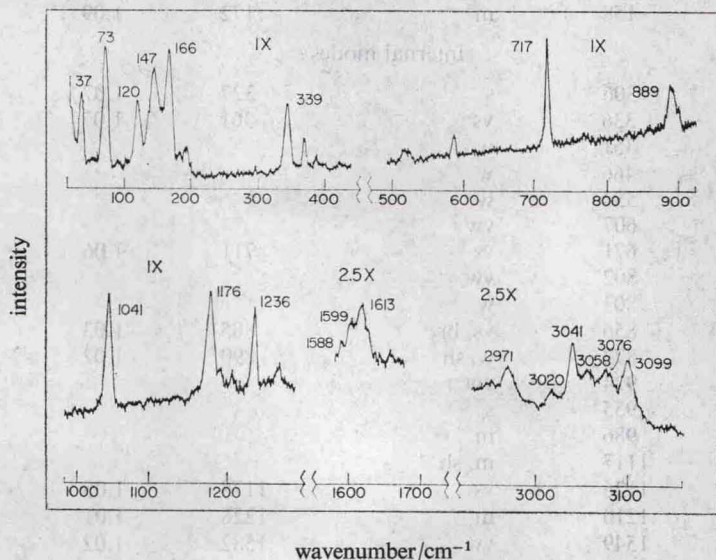
FIG. 5.—Raman spectrum of dianthracene at 10 kbar and 296 K.

(table 2). Significant qualitative changes are noted in the high pressure spectrum of the lattice phonons, with the behaviour being attributed to differing pressure dependence of the vibrational modes. Fig. 6 shows that one mode, originally at 110 cm^{-1} (1 bar), separates from a mode at 101 cm^{-1} (1 bar), sweeps across the peak at 133 cm^{-1} (1 bar), and finally appears as a high frequency shoulder of the 133 cm^{-1} peak. This implies that the modes at 110 and 133 cm^{-1} are of different symmetry.

Another change in the lattice modes is observed for the weak doublet originally at 167 and 172 cm^{-1} which have equal intensity at 1 bar. The 172 cm^{-1} component of the doublet shifts with pressure at a slightly higher rate and also becomes stronger in intensity with pressure. The observed wavenumbers are plotted against pressure in fig. 7 and 8 for the modes centred around the ring carbon–carbon stretch (1582 to
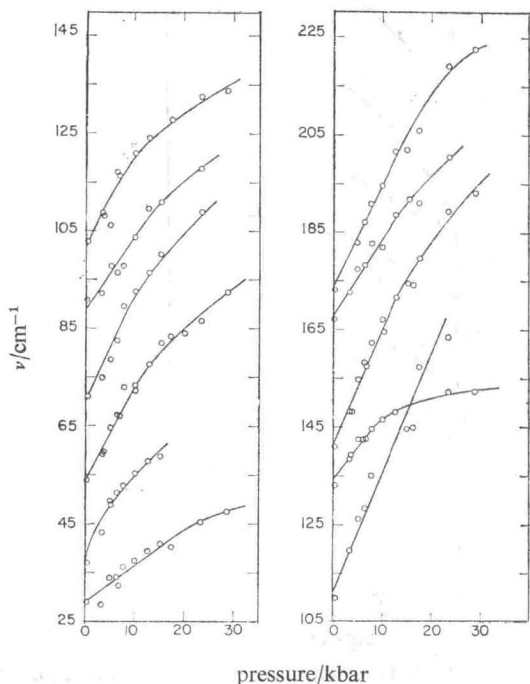
pressure/kbar

FIG. 6.—The wavenumbers for the lattice librational modes of dianthracene are plotted against pressure at 296 K.

pressure/kbar
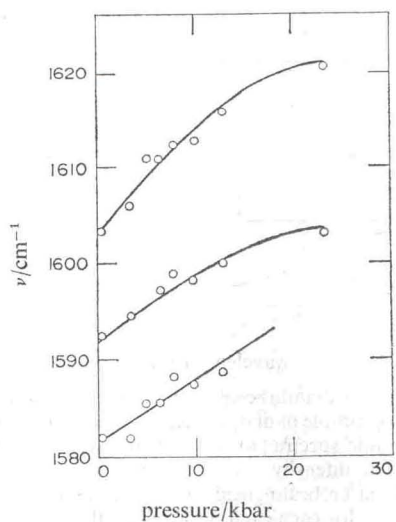
FIG. 7.—The wavenumbers for the internal modes centred around the C═H stretching band are plotted against pressure at 296 K.
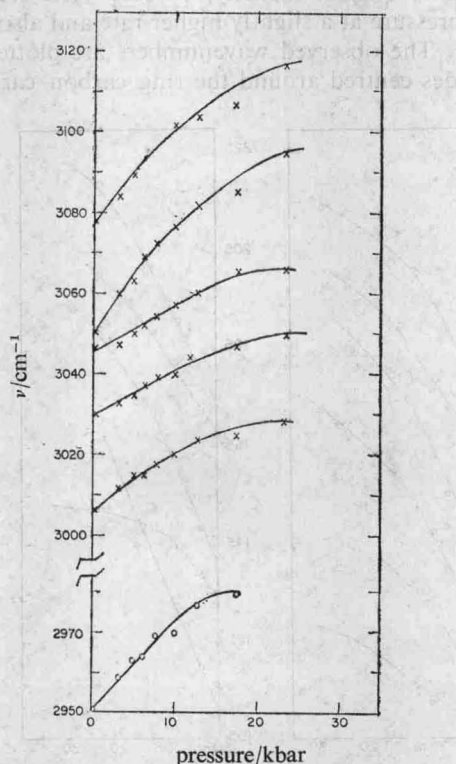
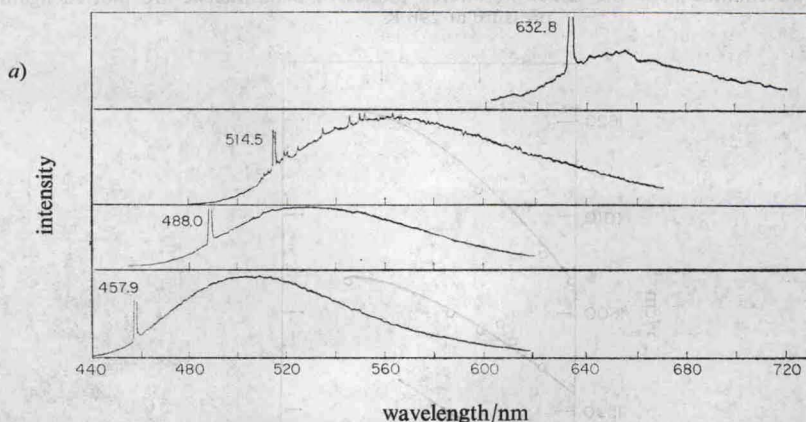FIG. 8.--A plot of the wavenumber shifts of the C—H stretching band against pressure at 296 K.

FIG. 9 —The luminescence spectra of dianthracene at 32 kbar and 300 K.   The above spectra (a)-(d) were taken on the same crystalline sample of dianthracene.   The spectrum (a) was excited at 632.8 nm using ~ 40 mW He–Ne laser, while spectra (b) to (d) were excited with the various Ar laser lines (514.5, 488.0 and 457.9 nm).   The intensity is arbitrary and there is no intensity correlation from spectrum to spectrum since the laser beam incident on the high pressure window was refocused for each exciting wavelength.

1603 cm^{-1}) and aliphatic (2951 cm^{-1}) and aromatic carbon–hydrogen stretch (3006 to 3078 cm^{-1})

When the dianthracene crystals were compressed and illuminated, for example at 514.5 nm and 296 K, a weak but broad luminescence background appeared around 10 kbar (fig. 5) and grew in intensity until at pressures higher than 25 kbar, the intensity was competitive to the Raman process.   Fig. 9 shows the structureless excimer-like luminescence excited with laser radiation at 457.9, 488.0, 514.5 and 632.8 nm.   At 32 kbar the emission is more intense than the dianthracene Raman spectra ; however, some of the stronger Raman peaks excited at 514.5 nm could still be followed.   The intensity of the emission band induced by pressure and irradiation decreased with decreasing excitation energy.   An interesting observation is that both pressure and irradiation appear to be required in creating high photoreactivity in dianthracene. The luminescence lifetime was determined to be approximately 10 ns at 25 kbar and 296 K when excited by 448.5 nm radiation.

DISCUSSION

The most significant conclusion of this study relates to the apparent *stability* of dianthracene.   The Raman spectra demonstrate that the dimer is quite stable under compression to 20 kbar and higher pressures, contrary to other reports.   No significant intensity of bands associated with the monomer and no obvious mode-instability or " softening " were observed.   One difference between these and other studies of the stability under compression was that crystals and compacted powder were used here whereas others have studied powder highly dispersed in compacted KBr matrices.[5, 7]   The shearing and exposure of a large surface area in preparation of KBr pellets may induce deomposition of the dimer, although this was not detected in the infrared spectra of dianthracene-KBr pellet shown in fig. 2.

The pressure dependences of the spectra of the lattice modes and many internal modes of dianthracene are qualitatively similar to those observed for benzene, naphthalene and anthracene.[23-25]   However, the shifts of the internal mode frequencies are especially large, by factors of 2 to 6.   It is especially interesting that the modes whose frequencies are most sensitive to pressure are the very low-frequency lattice modes and the very high-frequency aromatic C—H stretch modes.   This suggests that the predominant factor is the density dependence of the intermolecular H—H distances between atoms on the periphery of the molecules and the associated change of the intermolecular repulsive potentials.   Changes of intermolecular C—H distances also may contribute to this effect.   The relatively large magnitudes of these shifts suggests that the compressibility of dianthracene may be even larger than that of anthracene which, combined with the higher density of dianthracene at atmospheric pressure, implies that the relative stability of dianthracene is even greater at high pressures.[21]   This is consistent with the reported pressure–induced dimerization and polymerization of similar aromatic molecules.[26, 27]

The structureless and anomalous high pressure emission bands are a most puzzling feature of this work on dianthracene, and it is difficult to identify the emitting levels. The shape of each high pressure emission spectrum is very similar to one of the three reported excimer fluorescence spectra of dianthracene, namely the red-emitting or the " stable " and " unstable " green emitting sandwich dimers.[8, 28]   The high pressure emission band excited with the He–Ne laser (fig. 9), for example, is similar to the isolated red excimer fluorescence in crystalline dianthracene, while the spectra excited with the Ar ion laser (fig. 9) may be related to the green emitting sandwich dimer.   The measured fluorescence lifetime of 10 ns at 296 K and 25 kbar and excited by 448.5 nm radiation is not easily compared with the 77 K sandwich excimer lifetimes

of 215 and 10 ns for the " unstable " and " stable " green emitting and finally 110 ns for the red emitting sandwich dimers.[28-30] The fluorescence lifetime of the compressed dianthracene, however, is not inconsistent with the lifetimes of the excimer emissions at 77 K, since the latter are expected to be considerably shorter at ambient temperatures. It can be seen from the above discussion that the luminescence spectra of compressed dianthracene may arise from a distribution of close coupled sandwich-like defects that were created and trapped in the crystal under pressure. An alternate explanation is the occurrence of a high pressure phase transition in which another crystalline modification is formed.[31]

Further Raman and infrared studies of large single crystals of dianthracene would be desirable to explain the stability of the dimer. Polarization studies would be especially useful to establish the assignments of many of the Raman active peaks. The problem lies, however, in locating an appropriate solvent for dianthracene from which a large crystal could be grown.

[1] R. Luther and F. Weigert, *Z. phys. Chem.*, 1905, **51**, 297.
[2] E. J. Bowen and D. W. Tanner, *Trans. Faraday Soc.*, 1955, **51**, 473.
[3] M. O'Donnell, *Nature*, 1968, **218**, 460.
[4] P. C. Subudhi, N. Kanamuru and E. C. Lim, *Chem. Phys. Letters*, 1975, **32**, 503.
[5] E. J. Baum, *Photochemistry of Organic Solids: Anthracene, Excited State Chemistry*, ed. J. N. Pitts (Gordon and Breach, New York, 1970), p. 121.
[6] E. A. Chandross and J. Ferguson, *J. Chem. Phys.*, 1966, **45**, 3564.
[7] J. K. S. Wan, R. N. McCormick, E. J. Baum and J. N. Pitts, *J. Amer. Chem. Soc.*, 1965, **87**, 4409.
[8] E. A. Chandross, J. Ferguson and E. G. McRae, *J. Chem. Phys.*, 1966, **45**, 3546.
[9] P. F. Jones and M. Nicol, *J. Chem. Phys.*, 1968, **48**, 5440.
[10] K. N. Trueblood, *Molecular Dynamics and Structure of Solids*, ed. R. S. Carter and J. J. Rush (NBS publication 301, Washington, 1969), p. 355.
[11] J. M. Thomas and J. O. Williams, *Prog. Solid State Chem.*, 1971, **6**, 119.
[12] G. Adler, *Trans. Amer. Cryst. Assn.*, 1971, **7**, 55.
[13] G. Guarini and P. Sarti–Fantoni, *Mol. Cryst. Liquid Cryst.*, 1970, **6**, 423.
[14] M. Ehrenberg, *Acta Cryst.*, 1966, **20**, 177.
[15] M. M. Julian, *J.C.S. Dalton*, 1971, 558.
[16] R. L. Barnes and J. B. Birks, *Proc. Roy. Soc. A*, 1966, **291**, 570.
[17] B. Stevens, *Spectrochim. Acta*, 1962, **18**, 439.
[18] M. D. Cohen, Z. Ludmer and V. Yakhot, *Phys. Stat. Sol. B*, 1975, **67**, 51.
[19] J. Tanaka, T. Koda, S. Shinonoya and S. Minomura, *Bull. Chem. Soc. Japan*, 1965, **38**, 1559.
[20] H. Ohigashi, I. Shirotani, H. Inokuchi and S. Minomura, *Mol. Cryst.*, 1966, **1**, 463.
[21] M. Nicol, M. Vernon and J. T. Woo, *J. Chem. Phys.*, 1975, **63**, 1992.
[22] Infrared Spectrum of Anthracene, Sadtler Standard Spectra #1319 (Sadtler Research Laboratories, Philadelphia, Pa.).
[23] W. D. Ellenson and M. Nicol, *J. Chem. Phys.*, 1974, **61**, 1380 and references cited therein.
[24] D. A. Dows, L. Hsu, S. S. Mitra, O. Brafman, M. Hayek, W. B. Daniels and R. K. Crawford, *Chem. Phys. Letters*, 1973, **22**, 595.
[25] P. T. T. Wong and E. Whalley, *Rev. Sci. Instr.*, 1974, **45**, 904.
[26] R. B. Aust, W. H. Bentley and H. G. Drickamer, *J. Chem. Phys.*, 1964, **41**, 1856.
[27] M. Kuhlman and H. G. Drickamer, *J. Amer. Chem. Soc.*, 1972, **94**, 8325.
[28] J. Ferguson and A. W. H. Mau, *Mol. Phys.*, 1974, **27**, 377.
[29] P. E. Fielding and R. C. Jarnagen, *J. Chem. Phys.*, 1967, **47**, 247.
[30] N. Mataga, T. Torihashi and Y. Ota, *Chem. Phys. Letters*, 1967, **1**, 385.
[31] P. W. Bridgman, *Collected Experimental Papers* (Harvard University Press, Cambridge, Mass., 1964), vol. vi, p. 415.